Electronic Supplementary Information (ESI)

Octahedral morphology of NiO with (111) facet synthesized from the transformation of NiOHCl for NOx detection and degradation: Experiment and DFT calculation

Angga Hermawan[a,§], Adie Tri Hanindriyo[b,§], Erland Rachmad Ramadhan[c], Yusuke Asakura[a], Takuya Hasegawa[a], Kenta Hongo[c,d], Miki Inada[e], Ryo Maezono[c], and Shu Yin[a,*]

[a]Institute of Multidisciplinary research for Advanced Materials (IMRAM), Tohoku University 2-1-1 Katahira, Aoba-ku, Sendai, Miyagi 980-8577, Japan

[b]School of Materials Science, JAIST, Asahidai 1-1, Nomi, Ishikawa, 923-1292, Japan

[c]School of Information Science, JAIST, Asahidai 1-1, Nomi, Ishikawa, 923-1292, Japan

[d]Research Center for Advanced Computing Infrastructure, JAIST, Asahidai 1-1, Nomi, Ishikawa 923-1292, Japan

[e]Center of Advanced Instrumental Analysis, Kyushu University, 6-1 Kasuga-Koen, Kasuga-Shi, Fukuoka 816-8580, Japan

[§]The authors are equally contributed

*Corresponding author: Prof. Shu Yin email: yin.shu.b5@tohoku.ac.jp

Table of content

Text

Figures

Table

Text S1

NiO slab and NO_x adsorption model

NiO surface is modeled using slab models with a minimum of 4 atomic layers to approximate bulk effects to surfaces. Vacuum slabs between the 4 layers of NiO are used to prevent interaction with periodic images in the z-axis. Similarly, 2 × 2 surface unit cells (corresponding to 0.25 ML coverage) are used to prevent interaction between the NO adsorbate molecule and its periodic images in the x- and y-axes. Geometry optimization calculations are used to model adsorptions, with adsorbates situated initially at 2Å, from the surface adsorption site.

In order to ensure reliable calculations, the values of several calculation parameters are converged with respect to the total energy of the simulation cell. These parameters include the cut-off energy (in plane-wave DFT representing the size of the basis set used), the k-point grid for integrations (using Monkhorst-Pack grid),[1] and the aforementioned thickness of the vacuum slab. The calculations performed for this work uses a cut-off energy of 400 eV, a k-point grid of 5×5×1, and a vacuum slab of thickness 10 Å, converging the total energy of calculated systems to a reliability of 0.001 eV/atom. The antiferromagnetic ground state of NiO is also taken into account as initial magnetic moments for every calculation are set as antiferromagnetic in the [111] direction. Meanwhile, the adsorbate molecule NO is relatively much easier to model. Starting from the experimental work of Kukolich, the initial N-O bond length in vacuum was set as 1.154 Å.[2] Geometry optimization with the GGA-PBE exchange correlation functional slightly stretches the N-O bond length to 1.1692 Å, which is in good agreement with 1.16 Å from a previous ab initio work by Beheshtian et al.[3]

The surface energy is defined as the energy per area unit required to form a surface from the bulk material, and can be calculated as:

$$\sigma = \frac{1}{2S}\left(E^{N}_{surface} - N * E_{bulk}\right) \qquad \text{(Eq. 1)}$$

where N signifies the number of atoms making up the surface slab model, $E^{N}_{surface}$ the total energy of the slab model, E_{bulk} the total energy per atom of the bulk material and S signifies the area of the surface of the slab model (the factor of 2 shows the creation of 2 surfaces in a slab model. From

ab initio calculations, the surface energy of each low index NiO surface facet is calculated and displayed in Table I.

Table S1. Comparison of calculated surface energies σ of NiO surface facets

Facets	σ (J/m^2)	
	Absolute	Relative
(100)	0.864	0.000
(110)	1.949	+1.084
(111)	3.895	+3.031

The question of adsorption conformation is rather simple with the NO molecule as adsorbate, as only the orientation of the N-O bond needs to be considered. The two main geometric conformations considered are vertical and horizontal orientations, with respect to the NiO surface. In order to include the possibility of tilted orientations, the N-O bond is slightly tilted at about 10^o from the surface normal for vertical orientation initial atomic positions. Therefore, the geometry optimization algorithm can self consistently determine the energetically favorable final adsorption geometry without being "stuck" in any local minima which might occur due to symmetry from completely vertical adsorption. This allows the geometry optimization algorithm in VASP to converge to the final adsorption geometry from a reasonable initial atomic position, which in this work is set at 2Å above the surface.

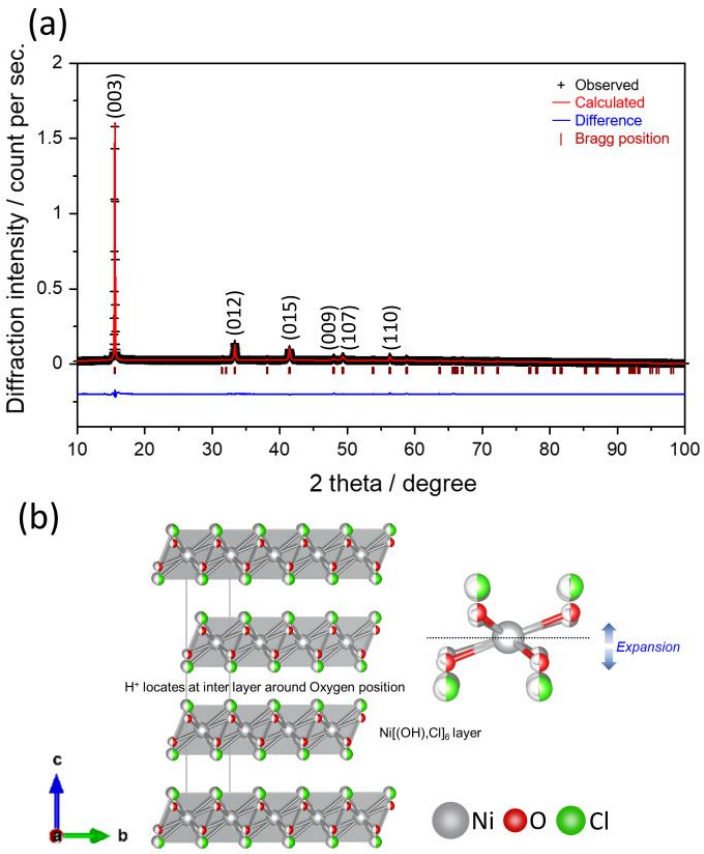

Fig. S1 (a) Rietveld refinement of powder X-Ray Diffraction (PXRD) and (b) crystal structures of NiOHCl after refinement

Table S2. Refined structural parameters of NiOHCl (space group = $R\bar{3}m$)

Atom	Wyckoff	Occ.	x	y	z	$U_{iso.}$ (nm^2)
Ni1	3a	1	0	0	0	0.043(1)
O1	6c	0.5	1/3	2/3	0.0448(8)	0.012(5)
Cl1	6c	0.5	1/3	2/3	0.0919(4)	0.023(2)

Table S3. Comparison of refined structural parameters of NiOHCl with earlier work

	This work	Reported[4]
Crystal system	Rhombohedral	
Space group	$R\bar{3}m$	
a (Å)	3.2674(1) [+0.2%]	3.26061(8)
c (Å)	17.068(1) [+0.3%]	17.00619(89)
V ($Å^3$)	157.80(1) [+0.8%]	156.57
Ni1	0	0
O1	0.0448(8)	0.03500(22)
Cl1	0.0919(4)	0.08790(8)
Ni-O (Å)	2.036(6)	1.9744(12)
Ni-Cl (Å)	2.453(5)	2.4038(9)

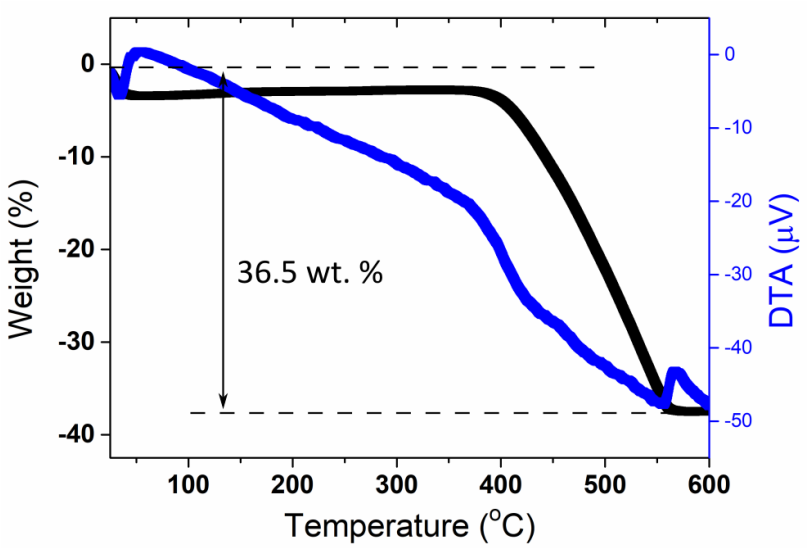

Fig. S2. TG/DTA curve of NiOHCl

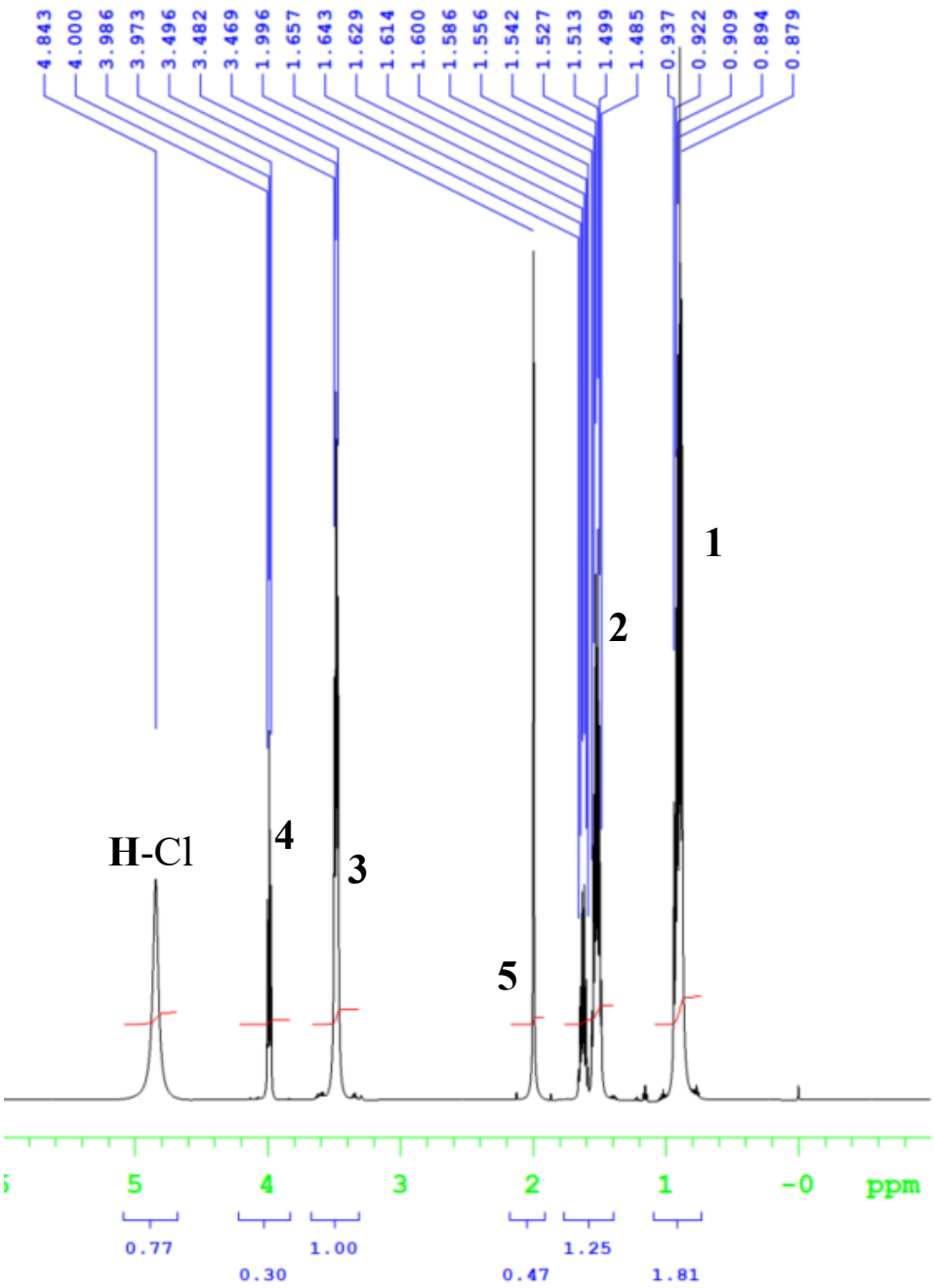

Fig. S3. NMR analysis from NiOHCl final solution synthesis

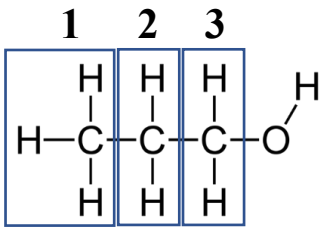

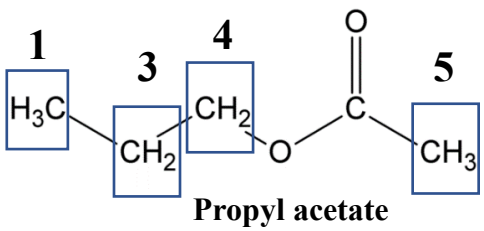

Text S2

NMR analysis

Herein, we performed ^{1}H NMR analysis to elucidate the chemical composition of solvents after the solvothermal process and propose the reaction pathway accordingly. In preparation for ^{1}H NMR measurement, the supernatant was diluted with deuterate CD_3OD. ^{1}H NMR spectrum (**Fig. S3**) indicates a signal of starting 1-propanol solution ($C\boldsymbol{H}_3CH_2CH_2OH$: 0.909 ppm, $CH_3C\boldsymbol{H}_2CH_2OH$: 1.513 ppm, $CH_3CH_2C\boldsymbol{H}_2OH$: and 3.482 ppm). In addition to these signals, we have detected the formation of propyl acetate ($C\boldsymbol{H}_3CH_2CH_2OOCCH_3$: 0.922 ppm, $CH_3CH_2C\boldsymbol{H}_2OOCCH_3$: 3.973 ppm, and $CH_3CH_2CH_2OOCC\boldsymbol{H}_3$: 1.995 ppm), dipropyl ether ($CH_3CH_2C\boldsymbol{H}_2OC\boldsymbol{H}_2CH_2CH_3$: 3.482 ppm, $CH_3C\boldsymbol{H}_2CH_2OCH_2C\boldsymbol{H}_2CH_3$: 1.586 ppm and $C\boldsymbol{H}_3CH_2CH_2OCH_2CH_2C\boldsymbol{H}_3$: 0.922 ppm) and hydrogen chloride ($\boldsymbol{H}$Cl: 4.84 ppm).[5] However, acetic acid signal was not detected, indicating it was fully reacted during the treatment. The presence of mixed chemicals provided direct evidence of the occurrence of esterification, dehydration, and hydrolysis. Thus, we propose a possible chemical pathway during the water-controlled release solvothermal process (WCRSP) based on the NMR analysis as shown in the reaction (Eq.1)-(Eq.3). At the first step, esterification reaction between 1-propanol and acetic acid, yielding certain amount of water molecules equal to the amount of acetic acid. The dehydration of 1-propanol also produced a small fraction of water molecules. Finally, these water molecules hydrolysed the $NiCl_2$ into NiOHCl. It might be suspected that propyl acetate plays a major role as structure-assisting surfactant by attaching to polar (003) planes inhibiting its growth along (003) planes, although the detailed mechanism is still uncertain at present moment, yet should be investigated in the future study.

$$CH_3CH_2CH_2OH + CH_3COOH \rightarrow CH_3CH_2CH_2OOCH_3 + H_2O \quad \text{(Eq. 1)}$$

$$CH_3CH_2CH_2OH \rightarrow CH_3CH_2CH_2OCH_2CH_2CH_3 + H_2O \quad \text{(Eq.2)}$$

$$NiCl_2 + 2H_2O \rightarrow NiOHCl + HCl \quad \text{(Eq.3)}$$

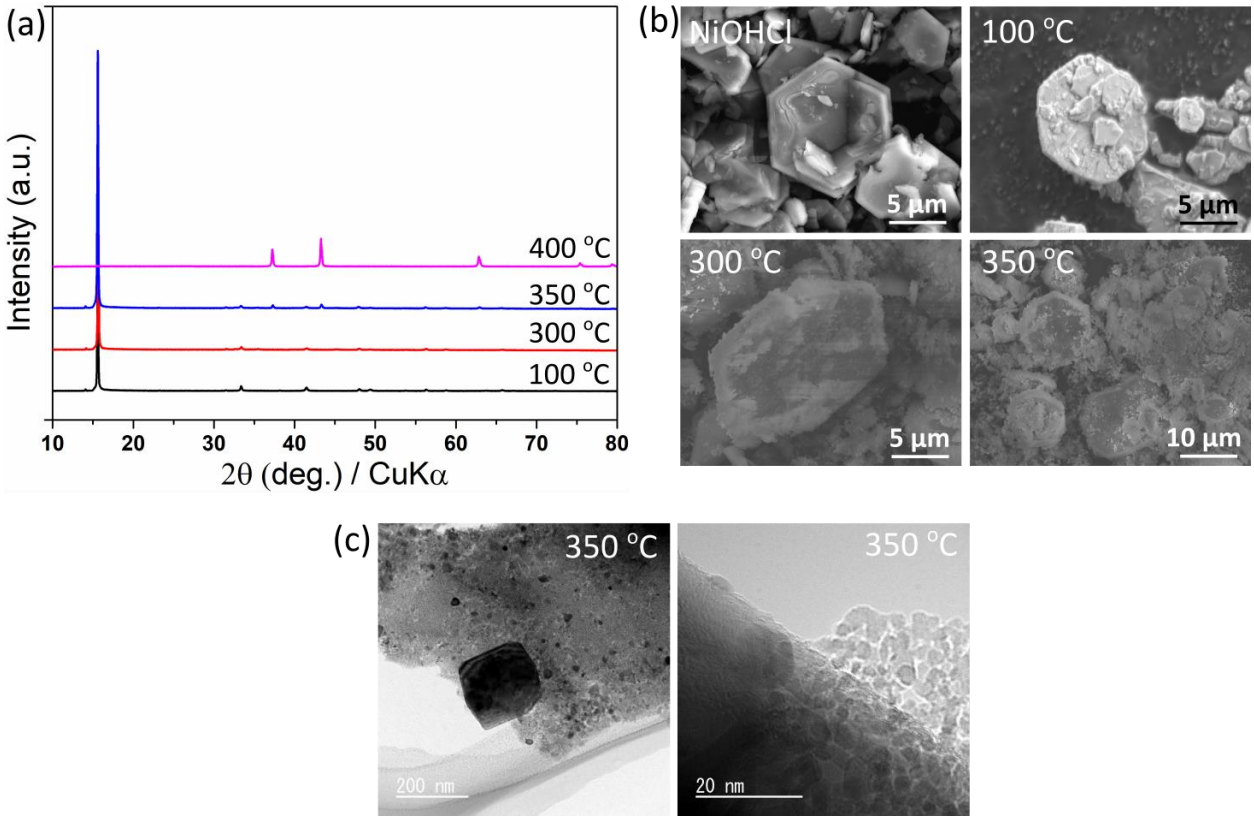

Fig. S4. (a) XRD patterns and (b) SEM image of NiOHCl calcined at elevated temperatures, and (c) HRTEM image of NiOHCl calcined at 350 ºC.

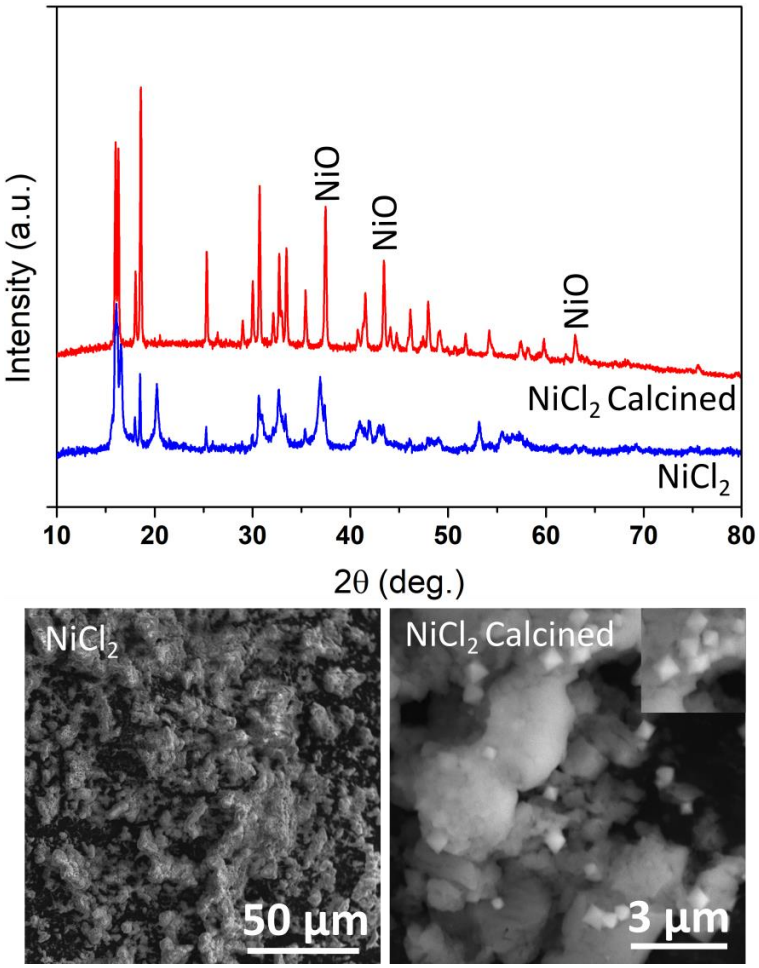

Fig. S5. XRD patterns and SEM image of $NiCl_2$ before and after calcination at 400 ^oC for 3h.

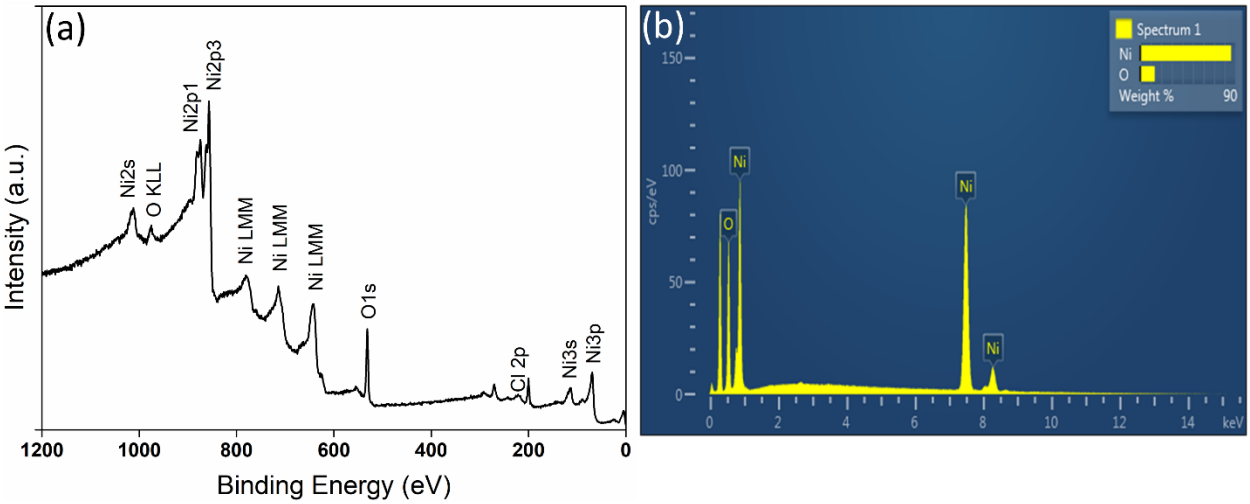

Fig. S6 (a) Full scan XPS spectra and (b) EDS spectra of NiO Octa (111)

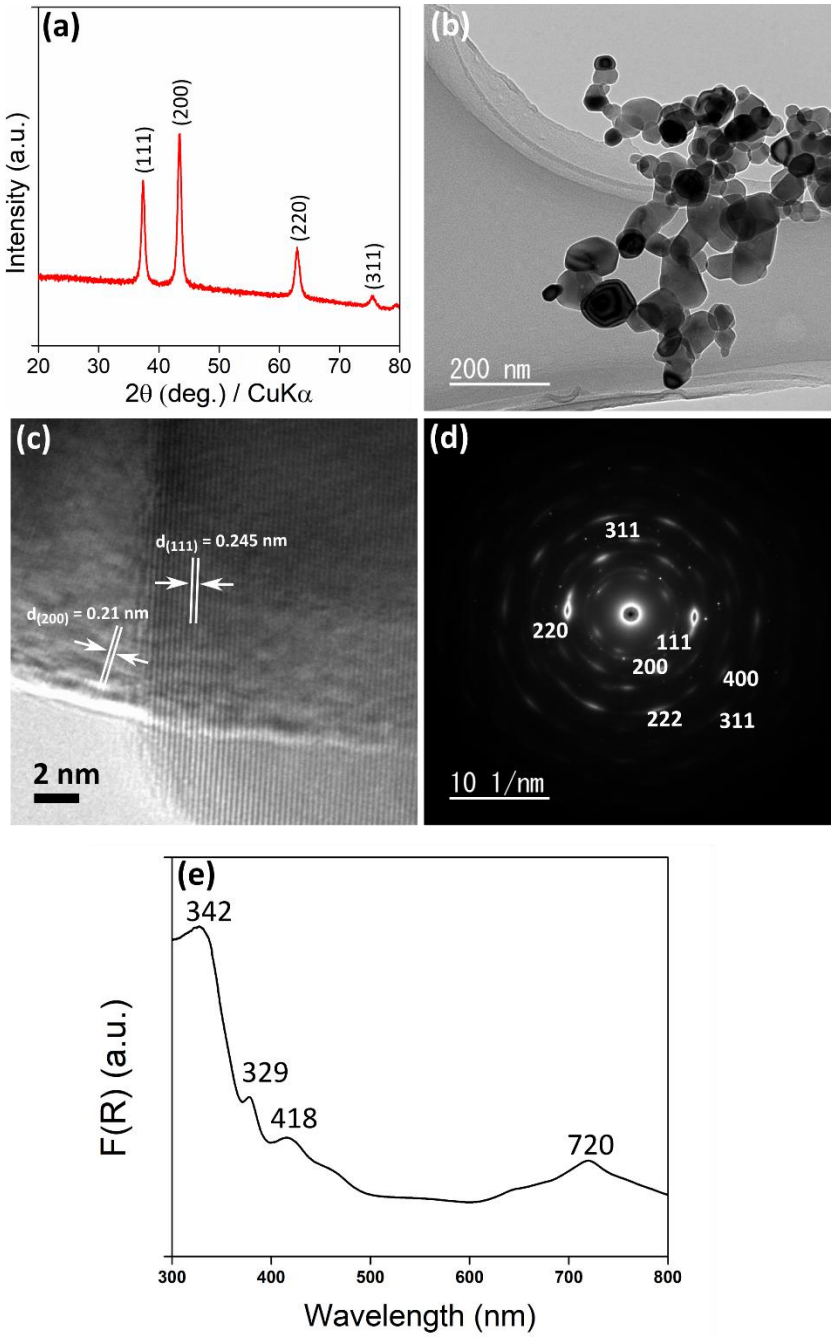

Fig. S7. (a) XRD pattern (b) TEM (c) HRTEM image (d) corresponding SAED pattern and (e) UV-Vis Absorption spectra of NiO irregular.

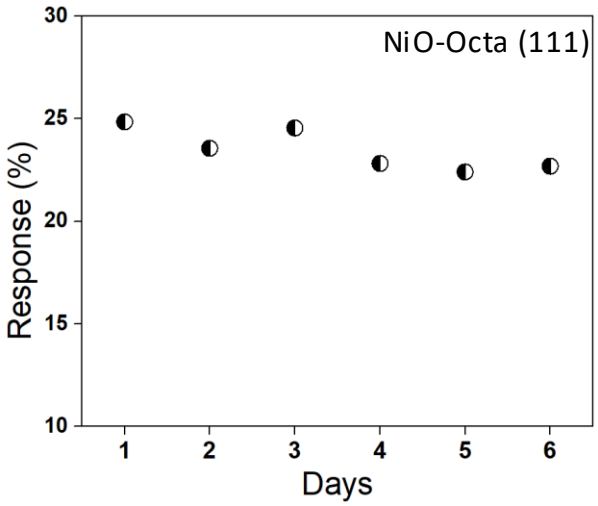

Fig. S8. Stability feature of NiO-Octa (111). NO_x gas sensing measurement was conducted for last 2 h each days. NO_x concentration was 3 ppm.

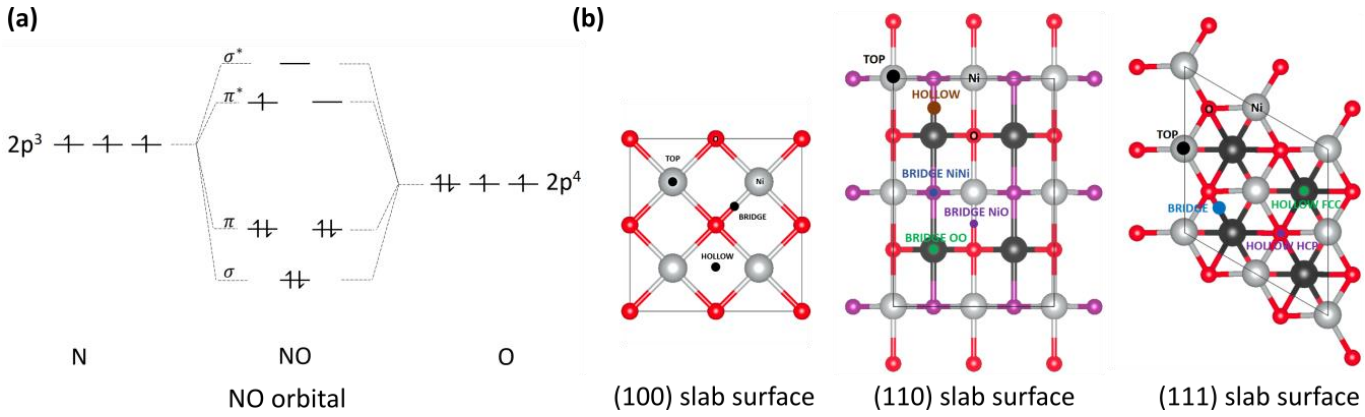

Fig. S9 (a) Diagram of NO molecular orbital as a result of hybridization between N and O 2p orbitals, (b) model of NiO (100), (110) and (111) slab surfaces. Gray and red are Ni and O atoms on the surface layer, while black and purple are Ni and O atoms are on the subsurface layer (subsubsurface layer for Ni atoms in (111) facet).

Table S4. NO adsorption on NiO (100), (110) and (111) surfaces

Surface	Conformation	E_{ads} (eV)
(100)	11_TopNiN	-0.150
	12_TopNiO	-0.134
	13_TopON	-0.182
	14_TopOO	-0.118
	21_HolN	-0.181
	22_HolO	-0.050
	31_BridN	-0.458
	32_BridO	-0.122
	33_BridPar	-0.423
(110)	11_TopNiN	-0.858
	12_TopNiO	-0.253
	13_TopON	-0.269
	14_TopOO	-0.086
	21_HolN	-1.231
	22_HolO	-0.110
	31_BridNiNiN	-1.248
	32_BridNiNiO	-0.087
	33_BridNiNiPar	-0.956
	34_BridOON	-0.145
	35_BridOOO	-0.109
	36_BridOOPar	-0.314
	37_BridNiON	-0.862
	38_BridNiOO	-0.235
	39_BridNiOPar	-0.870
(111)	11_TopN	-2.345
	12_TopO	-1.125
	21_HolFCCN	-1.915
	22_HolFCCO	-0.527
	23_HolHCPN	-2.429
	24_HolHCPO	-0.922
	31_BridN	-2.395
	32_BridO	-0.973
	33_BridPar	-2.094

Reference

1 H. J. Monkhorst and J. D. Pack, Special points for Brillouin-zone integrations, *Phys. Rev. B*, 1976, **13**, 5188–5192.

2 S. G. Kukolich, Structure of the NO Dimer, *J. Am. Chem. Soc.*, 1982, **104**, 4715–4716.

3 J. Beheshtian, M. Kamfiroozi, Z. Bagheri and A. Ahmadi, Computational study of CO and NO adsorption on magnesium oxide nanotubes, *Phys. E Low-Dimensional Syst. Nanostructures*, , DOI:10.1016/j.physe.2011.09.016.

4 S. Bette, R. E. Dinnebier and D. Freyer, Structure solution and refinement of stacking-faulted NiCl(OH), *J. Appl. Crystallogr.*, 2015, **48**, 1706–1718.

5 H. E. Gottlieb, V. Kotlyar and A. Nudelman, NMR chemical shifts of common laboratory solvents as trace impurities, *J. Org. Chem.*, 1997, **62**, 7512–7515.